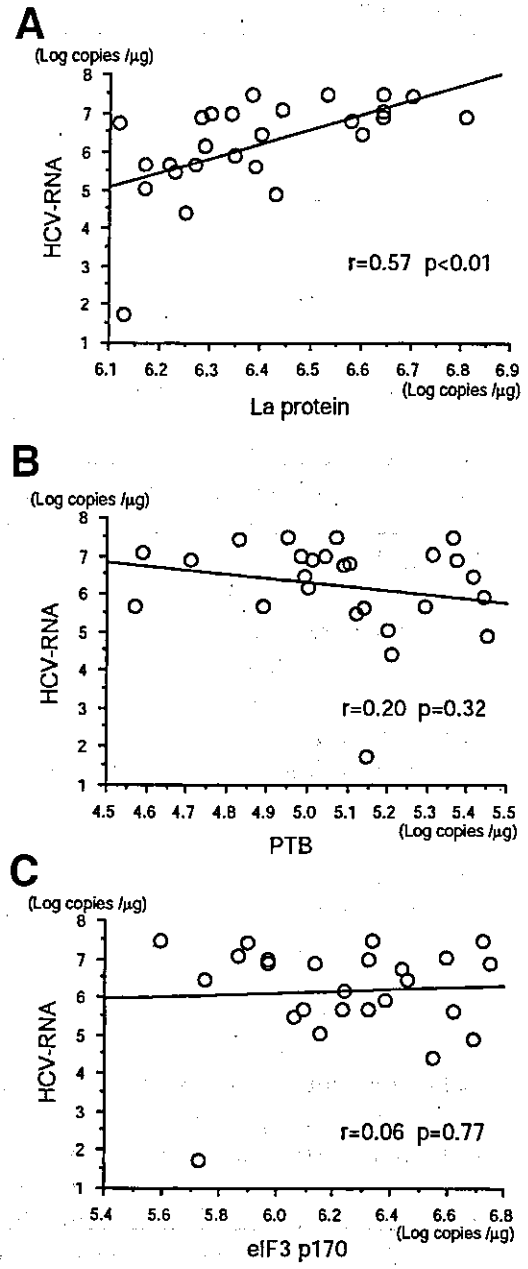


**Figure 9.** Correlation of La protein (*A*), PTB (*B*), and eIF3 p170 (*C*) with the amount of HCV RNA in tissue lesions of chronic hepatitis C.

the suppressed and overexpressed states. However, neither suppression nor overexpression of ribosomal protein S9 affected HCV IRES activity. Thus, this study could not identify the functional significance of ribosomal protein S9 for HCV IRES activity.

The definition of these initiation factors has very important clinical relevance to HCV replication. We therefore investigated the expression of La protein, PTB, and eIF3 in tissue lesions from patients with chronic hepatitis C. Expression of La protein was significantly increased in the liver of patients, whereas that of PTB and eIF3 did not significantly increase. Neither histological activity nor stage was associated, but the amount of liver HCV RNA was significantly correlated with the level of La protein expression. Patients that expressed high levels of La protein in the liver were infected with more HCV (Figure 10). Thus, La protein plays an important role in HCV replication in livers of patients with chronic hepatitis C. Two possible mechanisms might explain the induction of La protein in the livers of chronic hepatitis C patients. First, significant proportions of cells undergo division during hepatocyte regeneration, and the proportion of cells in M phase that lead to the induction of the La protein increases. Second, HCV induces La protein. Because the expression of PTB and eIF3 was not significantly induced in the tissue lesions of chronic hepatitis C patients in this study, there must be unknown mechanisms by which HCV infection induces La protein. Our preliminary results showed that HCV proteins increased La protein in Huh-7 cells (data not shown). Further analysis is needed to show the interaction between La protein induction and HCV replication in chronic hepatitis C.

In conclusion, we discovered host factors that regulate HCV translation and replication in the liver. The implication of these findings with regard to the HCV life cycle is shown in Figure 11. Hepatitis and the resulting increased regeneration of hepatocytes increase IRES activity and enhance HCV replication. This may be an important mechanism by which HCV maintains its viral load under host defense immune pressure. These findings shed new light on the mechanism of HCV replication and could be the basis for developing a novel antiviral therapy. Although La protein and PTB have been shown to be involved in the cell-cycle regulation of HCV IRES activity, many other host factors might also be involved.

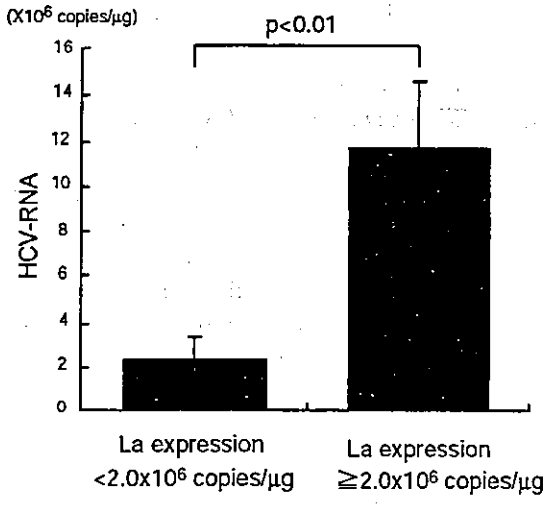


**Figure 10.** La protein expression and HCV RNA in liver.

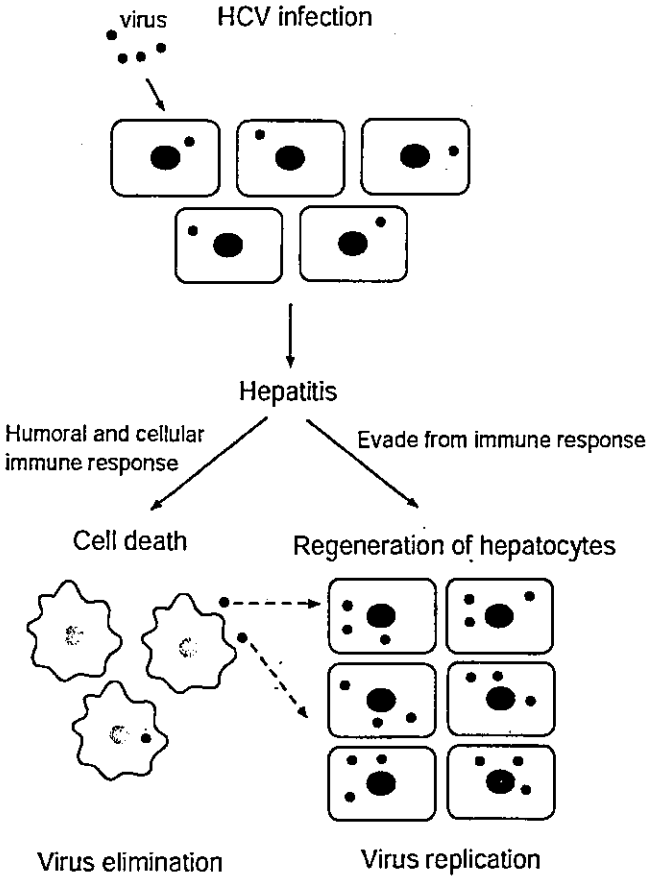


**Figure 11.** Hepatitis and HCV life cycle.

We are extending these analyses to other initiation factors and investigating the functional role on HCV IRES activity and replication of HCV.

## References


1. Choo QL, Kuo G, Weiner AJ, Overby LR, Bradley DW, Houghton M. Isolation of a cDNA clone derived from a blood-borne non-A, non-B viral hepatitis genome. Science 1989;244:359–362.
2. Kiyosawa K, Sodeyama T, Tanaka E, Gibo Y, Yoshizawa K, Nakano Y, Furuta S, Akahane Y, Nishioka K, Purcell RH, et al. Interrelationship of blood transfusion, non-A, non-B hepatitis and hepatocellular carcinoma: analysis by detection of antibody to hepatitis C virus. Hepatology 1990;12:671–675.
3. Davies MV, Pelletier J, Meerovitch K, Sonenberg N, Kaufman RJ. The effect of poliovirus proteinase 2Apro expression on cellular metabolism. Inhibition of DNA replication, RNA polymerase II transcription, and translation. J Biol Chem 1991;266: 14714–14720.
4. McHutchison JG, Gordon SC, Schiff ER, Shiffman ML, Lee WM, Rustgi VK, Goodman ZD, Ling MH, Cort S, Albrecht JK. Interferon alfa-2b alone or in combination with ribavirin as initial treatment for chronic hepatitis C. Hepatitis Interventional Therapy Group. N Engl J Med 1998;339:1485–1492.
5. Poynard T, Marcellin P, Lee SS, Niederau C, Minuk GS, Ideo G, Bain V, Heathcote J, Zeuzem S, Trepo C, Albrecht J. Randomised trial of interferon alpha2b plus ribavirin for 48 weeks or for 24 weeks versus interferon alpha2b plus placebo for 48 weeks for treatment of chronic infection with hepatitis C virus. International Hepatitis Interventional Therapy Group (IHIT). Lancet 1998;352:1426–1432.
6. Fried MW, Shiffman ML, Reddy KR, Smith C, Marinos G, Goncales FL Jr, Haussinger D, Diago M, Carosi G, Dhumeaux D, Craxi A, Lin A, Hoffman J, Yu J. Peginterferon alfa-2a plus ribavirin for chronic hepatitis C virus infection. N Engl J Med 2002;347:975–982.
7. Pestova TV, Shatsky IN, Fletcher SP, Jackson RJ, Hellen CU. A prokaryotic-like mode of cytoplasmic eukaryotic ribosome binding to the initiation codon during internal translation initiation of hepatitis C and classical swine fever virus RNAs. Genes Dev 1998;12:67–83.
8. Wang C, Sarnow P, Siddiqui A. Translation of human hepatitis C virus RNA in cultured cells is mediated by an internal ribosome-binding mechanism. J Virol 1993;67:3338–3344.
9. Reynolds JE, Kaminski A, Kettinen HJ, Grace K, Clarke BE, Carroll AR, Rowlands DJ, Jackson RJ. Unique features of internal initiation of hepatitis C virus RNA translation. EMBO J 1995;14:6010–6020.
10. Lu HH, Wimmer E. Poliovirus chimeras replicating under the translational control of genetic elements of hepatitis C virus reveal unusual properties of the internal ribosomal entry site of hepatitis C virus. Proc Natl Acad Sci U S A 1996;93:1412–1417.
11. Honda M, Ping LH, Rijnbrand RC, Amphlett E, Clarke B, Rowlands D, Lemon SM. Structural requirements for initiation of translation by internal ribosome entry within genome-length hepatitis C virus RNA. Virology 1996;222:31–42.
12. Wang C, Sarnow P, Siddiqui A. A conserved helical element is essential for internal initiation of translation of hepatitis C virus RNA. J Virol 1994;68:7301–7307.
13. Rijnbrand RC, Abbink TE, Haasnoot PC, Spaan WJ, Bredenbeek PJ. The influence of AUG codons in the hepatitis C virus 5′ nontranslated region on translation and mapping of the translation initiation window. Virology 1996;226:47–56.
14. Honda M, Brown EA, Lemon SM. Stability of a stem-loop involving the initiator AUG controls the efficiency of internal initiation of translation on hepatitis C virus RNA. RNA 1996;2:955–968.
15. Honda M, Beard MR, Ping LH, Lemon SM. A phylogenetically conserved stem-loop structure at the 5′ border of the internal ribosome entry site of hepatitis C virus is required for cap-independent viral translation. J Virol 1999;73:1165–1174.
16. Ali N, Siddiqui A. The La antigen binds 5′ noncoding region of the hepatitis C virus RNA in the context of the initiator AUG codon and stimulates internal ribosome entry site-mediated translation. Proc Natl Acad Sci U S A 1997;94:2249–2254.
17. Ali N, Pruijn GJ, Kenan DJ, Keene JD, Siddiqui A. Human La antigen is required for the hepatitis C virus internal ribosome entry site-mediated translation. J Biol Chem 2000;275:27531–27540.
18. Ali N, Siddiqui A. Interaction of polypyrimidine tract-binding protein with the 5′ noncoding region of the hepatitis C virus RNA genome and its functional requirement in internal initiation of translation. J Virol 1995;69:6367–6375.
19. Chung RT, Kaplan LM. Heterogeneous nuclear ribonucleoprotein I (hnRNP-I/PTB) selectively binds the conserved 3′ terminus of hepatitis C viral RNA. Biochem Biophys Res Commun 1999;254: 351–362.
20. Spangberg K, Schwartz S. Poly(C)-binding protein interacts with the hepatitis C virus 5′ untranslated region. J Gen Virol 1999; 80:1371–1376.
21. Sachs AB. Cell cycle-dependent translation initiation: IRES elements prevail. Cell 2000;101:243–245.
22. Honda M, Kaneko S, Matsushita E, Kobayashi K, Abell GA, Lemon SM. Cell cycle regulation of hepatitis C virus internal ribosomal entry site-directed translation. Gastroenterology 2000; 118:152–162.
23. Shimazaki T, Honda M, Kaneko S, Kobayashi K. Inhibition of internal ribosomal entry site-directed translation of HCV by re-

combinant IFN-alpha correlates with a reduced La protein. Hepatology 2002;35:199–208.
24. Gosert R, Chang KH, Rijnbrand R, Yi M, Sangar DV, Lemon SM. Transient expression of cellular polypyrimidine-tract binding protein stimulates cap-independent translation directed by both picornaviral and flaviviral internal ribosome entry sites in vivo. Mol Cell Biol 2000;20:1583–1595.
25. Siomi MC, Eder PS, Kataoka N, Wan L, Liu Q, Dreyfuss G. Transportin-mediated nuclear import of heterogeneous nuclear RNP proteins. J Cell Biol 1997;138:1181–1192.
26. Wang X, Liebhaber SA. Complementary change in cis determinants and trans factors in the evolution of an mRNP stability complex. EMBO J 1996;15:5040–5051.
27. Gaspar NJ, Kinzy TG, Scherer BJ, Humbelin M, Hershey JW, Merrick WC. Translation initiation factor eIF-2. Cloning and expression of the human cDNA encoding the gamma-subunit. J Biol Chem 1994;269:3415–3422.
28. Johnson KR, Merrick WC, Zoll WL, Zhu Y. Identification of cDNA clones for the large subunit of eukaryotic translation initiation factor 3. Comparison of homologues from human, *Nicotiana tabacum*, *Caenorhabditis elegans*, and *Saccharomyces cerevisiae*. J Biol Chem 1997;272:7106–7113.
29. Hanecak R, Brown-Driver V, Fox MC, Azad RF, Furusako S, Nozaki C, Ford C, Sasmor H, Anderson KP. Antisense oligonucleotide inhibition of hepatitis C virus gene expression in transformed hepatocytes. J Virol 1996;70:5203–5212.
30. Honda M, Kaneko S, Kawai H, Shirota Y, Kobayashi K. Differential gene expression between chronic hepatitis B and C hepatic lesion. Gastroenterology 2001;120:955–966.
31. Kruger M, Beger C, Li QX, Welch PJ, Tritz R, Leavitt M, Barber JR, Wong-Staal F. Identification of eIF2Bgamma and eIF2gamma as cofactors of hepatitis C virus internal ribosome entry site-mediated translation using a functional genomics approach. Proc Natl Acad Sci U S A 2000;97:8566–8571.
32. Buratti E, Tisminetzky S, Zotti M, Baralle FE. Functional analysis of the interaction between HCV 5'UTR and putative subunits of eukaryotic translation initiation factor eIF3. Nucleic Acids Res 1998;26:3179–3187.
33. Michel YM, Borman AM, Paulous S, Kean KM. Eukaryotic initiation factor 4G-poly(A) binding protein interaction is required for poly(A) tail-mediated stimulation of picornavirus internal ribosome entry segment-driven translation but not for X-mediated stimulation of hepatitis C virus translation. Mol Cell Biol 2001;21:4097–4109.
34. Cornelis S, Bruynooghe Y, Denecker G, Van Huffel S, Tinton S, Beyaert R. Identification and characterization of a novel cell cycle-regulated internal ribosome entry site. Mol Cell 2000;5:597–605.
35. Sachs AB, Sarnow P, Hentze MW. Starting at the beginning, middle, and end: translation initiation in eukaryotes. Cell 1997;89:831–838.
36. Kawai HF, Kaneko S, Honda M, Shirota Y, Kobayashi K. Alpha-fetoprotein-producing hepatoma cell lines share common expression profiles of genes in various categories demonstrated by cDNA microarray analysis. Hepatology 2001;33:676–691.
37. Shirota Y, Kaneko S, Honda M, Kawai HF, Kobayashi K. Identification of differentially expressed genes in hepatocellular carcinoma with cDNA microarrays. Hepatology 2001;33:832–840.
38. Takeuchi T, Katsume A, Tanaka T, Abe A, Inoue K, Tsukiyama-Kohara K, Kawaguchi R, Tanaka S, Kohara M. Real-time detection system for quantification of hepatitis C virus genome. Gastroenterology 1999;116:636–642.
39. Pestova TV, Kolupaeva VG, Lomakin IB, Pilipenko EV, Shatsky IN, Agol VI, Hellen CU. Molecular mechanisms of translation initiation in eukaryotes. Proc Natl Acad Sci U S A 2001;98:7029–7036.
40. Pflugheber J, Fredericksen B, Sumpter R Jr, Wang C, Ware F, Sodora DL, Gale M Jr. Regulation of PKR and IRF-1 during hepatitis C virus RNA replication. Proc Natl Acad Sci U S A 2002;99:7029–7036.

Received March 16, 2004. Accepted November 4, 2004.

Address requests for reprints to: Shuichi Kaneko, MD, PhD, Department of Gastroenterology, Graduate School of Medicine, Kanazawa University, Takara-Machi 13-1, Kanazawa, 920-8641, Japan. e-mail: skaneko@medf.m.kanazawa-u.ac.jp; fax: (81) 76-234-4250.

The authors thank Masami Ueda, Junko Hara, and Mikiko Nakamura for excellent technical assistance.

J Gastroenterol 2004; 39:873–878
DOI 10.1007/s00535-004-1404-z

Journal of Gastroenterology



# An open-label study of administration of EH0202, a health-food additive, to patients with chronic hepatitis C

KYOSUKE KAJI[1], SATOSHI YOSHIDA[2], NOBUO NAGATA[2], TATSUYA YAMASHITA[1], EISHIRO MIZUKOSHI[1], MASAO HONDA[1], YASUHIKO KOJIMA[2], and SHUICHI KANEKO[1]

[1]Department of Gastroenterology, Kanazawa University Hospital, Ishikawa, Japan
[2]Institute for Consumer Healthcare, Consumer Healthcare Division, Yamanouchi Pharmaceutical Co., Ltd., Tokyo, Japan

***Background.*** In this study, we examined the effect of EH0202, a mixture of four herbal extracts that are known to induce interferons, on hepatitis C virus (HCV)-RNA levels in patients with chronic hepatitis C. ***Methods.*** This was an open-label uncontrolled study. The study subjects ingested food containing EH0202 daily for 3 months, which was equivalent to 1 g of desiccated herbs daily. Clinical symptoms, hematology and biochemical examinations, urine, and HCV-RNA levels were examined before, during (1 month), and after the EH0202 treatment (3 months). ***Results.*** Among the 35 patients who successfully completed the study, there were improvements in malaise (seen in 6 patients before and in 2 after EH0202 treatment), bloating sensation in the abdomen (seen in 2 before and in none after treatment), and nausea and vomiting (seen in 2 before and in 1 after treatment). There were no changes in hematology or biochemical examination parameters. There was a statistically significant decrease in HCV-RNA levels in patients with high viral titers after 3 months of EH0202 administration. No serious adverse events were observed with the EH0202 treatment. ***Conclusions.*** These findings suggest that EH0202 may be safe and useful in the treatment of patients with chronic hepatitis C. Further studies are, however, needed to obtain a definitive conclusion.

**Key words:** hepatitis C, health food, food additive, HCV-RNA, interferon

## Introduction

In recent years, the number of people who use health foods has been increasing, reflecting an increase in public awareness of diet and fitness for improving health. However, there have been few clinical studies that evaluated the safety and efficacy of these health-food products.

EH0202 is a health-food additive that was developed by Yamanouchi Pharmaceutical Co., Ltd. (Tokyo, Japan). It is a mixture of four herbal extracts (see below) that are known to stimulate macrophage activity. Dr. Yasuhiko Kojima,[1] who was the first to describe interferon (IFN), in 1970, and who is one of the foremost experts in this field, together with his fellow researchers, has screened some 200 herbs commonly used as traditional Kampo (Chinese medicine) formulations in Japan. Based on their screening, four herbs were finally selected that were shown to be IFN inducers[2] and could be used as food additives. They were: pumpkin seeds (*Cucurbita moschata*), plantain seeds (*Plantago asiatica*), Japanese honeysuckle (*Lonicera japonica*), and safflower (*Carthamus tinctorius*). EH0202 is a mixture of these four extracts.

It has been shown that EH0202 administration decreases the incidence of viral pneumonia and the mortality rate in pigs with porcine reproductive and respiratory syndrome.[3] In addition, in postmenopausal women, oral EH0202 administration for 6 months improved subjective menopausal symptoms and increased granulocyte-macrophage colony-stimulating factor (GM-CSF) levels, while decreasing follicle-stimulating hormone (FSH) levels in blood. Thus, it appears that EH0202 acts to stimulate immunological systems and may improve endocrine dysfunction.[4]

IFNs have been used to treat patients with chronic hepatitis C, and, because EH0202 has been shown to stimulate macrophages and increase IFN levels in experimental animals, we examined the effect of EH0202

Received: September 19, 2003 / Accepted: February 13, 2004
*Reprint requests to:* S. Yoshida
*Present address:* Original Image Co., Ltd., Helios Kannai Bldg, 3-21-2 Motohama-cho, Naka-ku, Yokohama 231-0004, Japan

on hepatitis C virus (HCV)-RNA levels, clinical symptoms, and hematological and biochemical parameters in patients with chronic hepatitis C, in an open-label uncontrolled study.

## Methods

### *Patients*

The subjects included in the study were 50 patients with chronic hepatitis C (26 men and 24 women; 28–80 years old; mean ± SD, 59.0 ± 10.6 years old), who visited the Kanazawa University Hospital from February to November 2002. This study was carried out as an open-label study. Hepatitis C was diagnosed by the referring physicians, and the patients included in the study were those who agreed, in writing, to participate in the study. HCV serotypes were: group 1 (40 patients), group 2 (9 patients), and unknown (1 patient). Twenty-four patients had a history of receiving IFN therapy in the past.

After completion of the study, 15 of the 50 patients were excluded from the efficacy analysis for one of the following reasons: inappropriate dosage and/or administration (4 patients), data missing (4 patients), IFN had been administered during the 6 months prior to the commencement of administration of EH0202 (3 patients), premature discontinuation of EH0202 administration (2 patients), administration of IFN commenced during the EH0202 dosing period (1 patient), and a complication (hepatic tumor) was observed prior to administration (1 patient). Thus, efficacy was examined based on the data of 35 evaluable subjects (17 men and 18 women; 28–80 years old; mean ± SD, 60.5 ± 10.4 years). The number of patients classified based on the HCV serotype was 27 patients for group 1, 7 patients for group 2, and 1 patient, unclassified. Of the 35 evaluable patients, 15 patients had a previous history of receiving IFN therapy. The 15 patients excluded from the efficacy evaluation of EH0202, who nonetheless, took EH0202, were included in the safety analysis, together with the 35 evaluable patients.

During the EH0202 treatment period, concomitant medications for the liver conditions were used in 22 patients. Thirteen patients had received ursodeoxycholic acid prior to and during the study. During EH0202 treatment, 5 patients started to take ursodeoxycholic acid for the first time. A glycyrrhizin preparation was used in conjunction with ursodeoxycholic acid in 2 patients, and in conjunction with Kantec (malotilate; Daiichi Pharmaceutical, Tokyo, Japan) and Proheparum S (liver hydrolysate; Kaken Pharmaceutical, Tokyo, Japan) tablets in 1 patient. Taurine powder was used in conjunction with ursodeoxycholic acid in 1 patient. Aminoleban (a branch-chained amino acids; Otsuka Pharmaceutical, Tokyo, Japan), Shosaiko-to (a bupleurum root-based formula; Tsumura, Tokyo, Japan), and Proheparum tablets were used as single agents in 1 patient each.

### *Test product*

In this study, we used InterPunch (Sanwell, Tokyo, Japan), a commercially available form of EH0202, as the test product. EH0202 is a mixture of four herbal extracts: *Cucurbita moschata* (seeds), *Plantago asiatica* (mature seeds), *Lonicera japonica* (flowers and flower buds), and *Carthamus tinctorius* (dried tubular flowers). These herbs were dried and weighed and then added to water equal to ten times the total weight of the dried herbs. The mixture was heated for 30 min at 95 ± 5°C in order to prepare an extract. The extract was strained and condensed. Inactive ingredients and flavors, such as lactulose, maltitol, lactose, and starch, were added to the extract. The mixture was then formed into fine granules. Finally, the granules and *Bifidobacterium longum* were combined to prepare the product. Two packets of InterPunch (1.5 g × 2 packets), which is the daily dosage, contain the equivalent of 1 g of the dried herbs listed above.

### *Test parameters*

Six clinical symptoms, namely, nausea and vomiting, abdominal pain, a bloating sensation in the abdomen, hematemesis and hematochezia, pruritus, and malaise, were examined. The clinical symptoms were examined and recorded by physicians when each patient visited the hospital. The parameters in hematological examinations were: white blood cell count, red blood cell count, hemoglobin, hematocrit, platelet count, and differential white blood cell count. The parameters in the biochemical examinations were: aspartate aminotransferase (AST), alanine aminotransferase (ALT), alkaline phosphatase, γ-guanosine triphosphate (GTP), Zincsulfate Turbidity Test (ZTT), lactic dehydrogenase (LDH), urea nitrogen, creatinine, Na, K, Cl, total bilirubin, total protein, albumin, total cholesterol, and triglycerides. Urinalysis parameters were protein, glucose, and occult blood. HCV-RNA levels were quantified, using AMPLICOR version 2.0 assay (Roche Diagnostics, Tokyo, Japan). The HCV antibody titer was measured using Lumipulse II Ortho HCV (Ortho-Clinical Diagnostics, Tokyo, Japan); the standard upper limit is 850 KIU/ml in this assay. If the measurement was above this value, HCV-RNA was remeasured following appropriate dilution of the sample. These measurements were performed prior to and 1 month and 3 months following the commencement of administration of EH0202.

**Table 1.** Clinical symptoms

| | Number of patients (Total number, 35) | | |
|---|---|---|---|
| | At the start | 1 Month | 3 Months |
| Symptoms | | | |
| Malaise | 6 | 2 | 2 |
| Bloating sensation in the abdomen | 2 | 1 | 0 |
| Nausea/vomiting | 2 | 2 | 1 |
| Pruritus | 1 | 1 | 1 |

**Table 2.** Effects of EH0202 on hematological indices

| | Pre | 1 Month | 3 Months |
|---|---|---|---|
| White blood cell count ($\times 10^3$/mm$^3$) | 3.9 ± 1.2 | 3.9 ± 1.2 | 3.9 ± 1.2 |
| Red blood cell count ($\times 10^4$/mm$^3$) | 433 ± 53 | 431 ± 52 | 432 ± 50 |
| Hemoglobin (g/dl) | 13.6 ± 1.7 | 13.4 ± 1.6 | 13.4 ± 1.6 |
| Hematocrit (%) | 40.0 ± 4.6 | 39.6 ± 4.3 | 39.9 ± 4.3 |
| Platelet count ($\times 10^4$/mm$^3$) | 12.6 ± 5.1 | 12.5 ± 5.2 | 12.4 ± 5.1 |

Data values are presented as means ± SD ($n$ = 34 patients)

*Statistical analysis*

Data from hematological and biochemical examinations, HCV-RNA analyses, and the HCV antibody assays were analyzed by means of Student's $t$-test. The efficacy of concomitant medications was analyzed by means of the $\chi^2$ test.

## Results

*Clinical symptoms*

Malaise was observed in six patients prior to administration. At 1 month of administration, improvement was observed in four of the six patients (66.7%). Improvement was also observed in the same four patients after 3 months of administration (Table 1). Two patients had a bloating sensation in the abdomen, and improvement was observed in one of the two patients (50%) after 1 month of administration, and in both patients (100%) after 3 months of administration. Two patients had nausea and vomiting, and improvement was observed in one of the two patients (50%) after 3 months of administration.

*Blood and biochemical examinations, and urinalysis*

No change was observed in any hematological parameters, such as white blood cell (WBC) count, red blood cell count, hemoglobin, hematocrit, and platelet count (Table 2). Administration of EH0202 did not influence WBC differentials (data not shown).

In biochemical examinations, ZTT was 17.5 ± 7.6 IU/l prior to administration, while it was 18.4 ± 7.8 IU/l after 3 months of administration. The increase was significant ($P < 0.05$). Na was 141.5 ± 2.2 mEq/l prior to administration, while it was 142.7 ± 2.0 mEq/l after 1 month of administration. This increase was also significant ($P < 0.01$). However, serum Na concentration after 3 months of administration was similar to the value prior to administration (141.1 ± 2.2 mEq/l). Parameters that indicate the level of hepatic and/or renal function did not change during the study (Table 3). No change was observed in the hematological or biochemical indices following the cessation of EH0202 administration. No significant change was observed in urinalysis findings.

*HCV-RNA quantification and HCV antibody titer*

Average HCV-RNA levels for the 35 patients were 734.4 ± 716.1 KIU/ml, 605.1 ± 471.1 KIU/ml, and 578.7 ± 437.9 KIU/ml prior to and 1 month and 3 months following the commencement of EH0202 administration, respectively (means ± SD). Although HCV-RNA levels tended to decrease with time, the decrease was statistically insignificant.

Further analysis was conducted by classifying patients into one of four groups, based on their baseline HCV-RNA, i.e., below 100 KIU/ml, 100–499 KIU/ml, 500–849 KIU/ml, and over 850 KIU/ml. As shown in Fig. 1, HCV-RNA levels had decreased significantly after 1 and 3 months of administration in patients in the over-850-KIU/ml group ($n$ = 12; $P$ = 0.044 and $P$ = 0.024,

**Table 3.** Effects of EH0202 on biochemical indices

| | *n* | Pre | 1 Month | 3 Months |
|---|---|---|---|---|
| AST (IU/l) | 35 | 59.7 ± 29.2 | 61.1 ± 30.2 | 57.4 ± 28.5 |
| ALT (IU/l) | 35 | 70.6 ± 39.6 | 68.9 ± 37.9 | 66.4 ± 35.4 |
| Alkaline phosphatase (IU/l) | 35 | 335.1 ± 162.0 | 341.4 ± 168.9 | 342.9 ± 170.7 |
| γ-GTP (IU/l) | 35 | 53.9 ± 53.8 | 52.7 ± 48.8 | 50.6 ± 35.8 |
| ZTT (IU/l) | 34 | 17.5 ± 7.6 | 17.6 ± 7.3 | 18.4 ± 7.8* |
| LDH (IU/l) | 35 | 199.4 ± 41.4 | 198.2 ± 35.4 | 193.8 ± 31.6 |
| Total bilirubin (mg/dl) | 35 | 0.8 ± 0.3 | 0.8 ± 0.3 | 0.8 ± 0.4 |
| Total protein (g/dl) | 35 | 7.4 ± 0.5 | 7.4 ± 0.4 | 7.3 ± 0.5 |
| Albumin (g/dl) | 34 | 4.3 ± 0.5 | 4.26 ± 0.45 | 4.3 ± 0.4 |
| Urea nitrogen (mg/dl) | 34 | 15.9 ± 4.6 | 16.7 ± 4.4 | 15.9 ± 4.1 |
| Creatinine (mg/dl) | 34 | 0.7 ± 0.2 | 0.7 ± 0.2 | 0.7 ± 0.2 |
| Na (mEq/l) | 34 | 141.5 ± 2.2 | 142.7 ± 2.0** | 141.1 ± 2.2 |
| K (mEq/l) | 34 | 4.1 ± 0.4 | 4.2 ± 0.4 | 4.2 ± 0.4 |
| Cl (mEq/l) | 34 | 105.2 ± 2.4 | 105.9 ± 2.3 | 104.6 ± 2.2 |
| Total cholesterol (mg/dl) | 33 | 174.5 ± 38.5 | 172.9 ± 34.0 | 170.0 ± 33.8 |
| Triglycerides (mg/dl) | 33 | 104.9 ± 50.3 | 96.1 ± 42.2 | 107.6 ± 62.3 |

*$P < 0.05$; **$P < 0.01$ vs Pre
Data values are presented as means ± SD

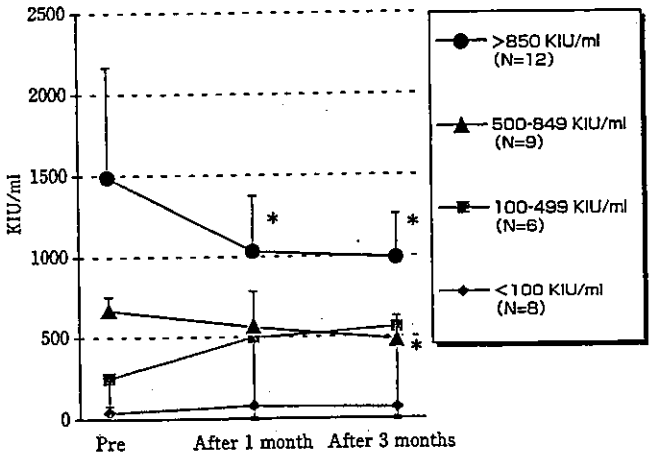


**Fig. 1.** Hepatitis C virus (HCV)-RNA levels were quantified using the AMPLICOR version 2.0 assay (Roche Diagnostics, Tokyo, Japan). Values represent means ± SD. *$P < 0.05$, Compared to the pretreatment value

respectively). HCV-RNA had also decreased significantly after 3 months of administration in patients in the 500- to 849-KIU/ml group ($n = 9$; $P = 0.021$). In general, no significant change was observed in patients with HCV-RNA levels below 500 KIU/ml, except for one patient who had a level of HCV-RNA of 1.4 KIU/ml before administration, with a level below the detection limit after 1 month of EH0202 administration. The level in this patient remained below the detection limit both at 1 month and 3 months after the cessation of the administration. We also tried to collect data on viral RNA levels after the study, but it was virtually impossible to collect useful data, because patients were treated with various drugs and regimens, including IFN.

A statistical analysis of the HCV antibody titer was carried out. Complete sets of antibody data were available only for 25 patients. The HCV antibody titer was 66.44 ± 7.78 HCV-Ab index, 67.17 ± 7.00 HCV-Ab index, and 66.83 ± 8.23 HCV-Ab index prior to and at 1 month and 3 months of administration, respectively. That is, no change was observed in the HCV antibody titer following EH0202 treatment. Further analysis by group, as specified above, did not show significant change either.

No significant correlation between HCV-RNA and AST/ALT was observed in patients whose HCV-RNA decreased significantly. In addition, we performed the $\chi^2$ test in order to analyze the difference, with respect to changes in HCV-RNA, between patients using concomitant drugs and patients not using concomitant drugs. The difference, with respect to changes in HCV-RNA, between patients using ursodeoxycholic acid, which was the most commonly used concomitant drug in this study, and patients not using ursodeoxycholic acid was also analyzed. In all cases, no significant difference was observed. No particular trend was observed between improvement in clinical signs/symptoms and the amount of virus.

*Adverse events*

A 71-year-old female patient had mild diarrhea in the first month of the dosing period, but the diarrhea disappeared with continued use of EH0202. A 60-year-old male patient experienced a mild bloating sensation in the abdomen during the third month of the dosing period, which did not call for termination of EH0202 treatment. No other adverse events were observed.

## Discussion

Currently there are 4 million patients with viral hepatitis in Japan. In addition, it is thought that there are more than 1 million carriers of HCV.[5] In the United States, it is known that 4 million people have been infected with HCV.[6] Thus, hepatitis is a major international health problem which requires significant medical attention.

The general strategies for the treatment of chronic hepatitis C are to eradicate HCV and to suppress hepatitis. IFNs are the mainstay in the treatment of hepatitis C by eradicating HCV; however, complete responses are not always obtained, and the treatment is not without side effects. More recently, a combination of IFN and ribavirin has been introduced as a better treatment of chronic hepatitis C; however, a complete response has yet to be seen, and this treatment is also associated with side effects such as granulocytopenia, thrombocytopenia, and flu-like symptoms.

The present study was an open-label, uncontrolled study of the effect of EH0202 in patients with chronic hepatitis C. In addition to the examination of clinical symptoms, quantification of hematological indices, biochemical examinations, and determination of HCV-RNA levels were made prior to and 1 month and 3 months after the commencement of EH0202 treatment. The most notable finding was a significant decrease in HCV-RNA levels, which was found in patients with viral titers higher than 500 KIU/ml. Namely, there was a statistically significant decrease in HCV-RNA in the 500- to 849-KIU/ml group, at 3 months, and in the over-850-KIU/ml group at 1 month and 3 months following EH0202 commencement ($P < 0.05$). In addition, a few patients showed improvement in certain clinical symptoms, but this was not found in all subjects.

It has been reported that the coefficients of variation of the version 2.0 AMPLICOR test range from 18% to 39%.[7] In our study, the amount of virus in patients with a high viral load (over 850 KIU/ml) decreased to 65.7% of the baseline value (on average, from 1447 KIU/ml to 951 KIU/ml) following the administration of EH0202, which fell within the range of the reported variation.[7] Thus, no definitive conclusion could be made from this study, and further studies are needed to clarify this question. It has been shown in animal studies that EH0202 promotes the phagocytic activity of macrophages (monocytes) in blood when it is administered to dairy cattle.[8] It has also been reported that EH0202 promotes the phagocytic activity of peritoneal macrophages and promotes IFN production in blood in mice following oral administration.[9] These findings in experimental animals suggest that EH0202 induces IFNs within the body, which may lead to an increase in antiviral activity.

Abnormally elevated levels of AST and ALT in patients with chronic hepatitis C were not decreased or influenced by EH0202 treatment, even in patients whose HCV-RNA levels were significantly decreased. Thus, there was no overt correlation between the amount of viral load and the indices of hepatic dysfunction. It has been reported that the prognosis of hepatic diseases depends on decreases in AST and ALT.[10] In contrast, it is not yet known if a decrease in viral load is directly correlated with clinical improvement in patients with hepatitis C. Nevertheless, the use of EH0202, either concomitantly with, or without other medications, may be effective in the treatment of hepatitis C, because a complete response to IFN treatment is known to depend critically on a decrease in the viral load. In addition, because hepatitis C virus is implicated not only in the inflammatory process in hepatitis but also in the carcinogenic process leading to the development of hepatoma,[11] it appears prudent to suppress the viral titer as much and for as long as possible.

With respect to clinical symptoms, even though relatively few patients experienced symptoms at the outset of the study, the improvements were notable. At 3 months of EH0202 administration, improvements were observed in four of the six patients who experienced malaise, in two of the two patients who had a bloating sensation in the abdomen, and in one of the two patients who had nausea/vomiting. No patient experienced exacerbation of the clinical symptoms that had been observed prior to administration during or after EH0202 treatment. These findings thus suggest that EH0202 may also contribute to improvements in quality of life (QOL), and if so, EH0202 may be a useful health-food additive with antiviral potency. However, further studies are needed to definitively prove this point, because the current study was an open-label uncontrolled study, which does not permit such conclusions.

In this study, two adverse events, both minor, were observed. One was mild diarrhea, which was observed during the first month of the dosing period. The patient recovered soon after, despite continuation of EH0202 administration, and it was therefore considered a transient reaction. Because InterPunch used in this study contains *Bifidobacterium longum*, the diarrhea may have been caused by this bacterium. The other adverse event was a mild bloating sensation in the abdomen, which was observed in a 60-year-old male patient during the third month of the dosing period, but it was mild and did not necessitate stopping EH0202 treatment. No other adverse event was observed in the 35 evaluable patients, or in the other 15 patients who did not qualify for evaluation of efficacy, but took EH0202 in the study. These findings suggest that oral administration of EH0202 daily for 3 months is not associated with any serious adverse event; thus, it can be considered safe.

It is known that IFNs can be toxic in high doses, as intensive IFN therapy greatly influences immunomodulation and causes adverse drug reactions that occur in the central nervous, endocrine, and/or digestive systems. In contrast to direct IFN therapy, indirect stimulation of IFN production in the body by various means has not been shown to cause any adverse events. Thus, the finding of no adverse events induced by EH0202 treatment is also consistent with the existing knowledge, and oral EH0202 treatment can be considered safe.

Our findings in this study suggest that oral EH0202 treatment may decrease the viral load in patients with chronic hepatitis C, as soon as 1 month after its administration is begun. The effect of EH0202 appears to be more dominant in patients with high viral titers than in those with a low titer. In some patients, EH0202 may also improve certain symptoms, such as malaise. That oral EH0202 treatment is safe was also shown by the lack of any serious adverse event associated with the treatment, and by the finding that parameters in the blood and biochemical examinations did not worsen. While it is clear that many more studies are necessary to clearly define the safety and the efficacy of EH0202, the preliminary findings in our present study suggest that EH0202 may be a useful health-food additive with antiviral activity to be used in the treatment of chronic hepatitis, such as hepatitis C, and it merits further investigation.

## References

1. Kojima Y. Sites of interferon production in rabbits induced by bacterial endotoxin. Kitasato Arch of Exp Med 1970;43:35–44.
2. Kojima Y. Kampo medicines and interferon inducers. Kampo Medicine 1981;5:9–15.
3. Toriumi H, Ichikawa Y, Terao T, Yamagiwa K, Shimizu K, Takeishi M, et al. Clinical efficacy of the feed additive MACH on the incidence of respiratory diseases in piglets. In: Proceedings of Guangzhou International Conference on the Advanced Traditional Chinese Veterinary Medicine '2000'; 2000 Oct 15–18; Guangzhou, China. South China Agricultural University, Guangzhou, China; 2000. p. 193–6.
4. Ushiroyama T, Yoshida S, Tadaki K, Ikeda A, Ueki M. A pilot study of a Kampo formula, EH0202, with intriguing results for menopausal symptoms. J Altern Complement Med 2004;10:397–9.
5. Satoh T. Report on a meeting of professionals to discuss combating hepatitis. Tokyo: Health Science Division, Minister's secretariat, Ministry of Health, Labour, and Welfare; March 30, 2001.
6. Alter MJ. Epidemiology of hepatitis C. Hepatology 1997;26:(Suppl 1):62S–5S.
7. Lee SC, Antony A, Lee N, Leibow J, Yang JQ, Soviero S, et al. Improved version 2.0 qualitative and quantitative AMPLICOR reverse transcription-PCR tests for hepatitis C virus RNA: calibration to international units, enhanced genotype reactivity, and performance characteristics. J Clin Microbiol 2000;38:4171–9.
8. Yoshida M, Tanemura K, Wakabayashi A, Otsuka Y, Yoshida S, Onda E, et al. Study of therapeutic effect of plant complex feed C-UP III on subclinical mastitis caused by *S. aureus* in dairy cows and activation of blood macrophage (in Japanese with English abstract). In: Proceedings of Pacific Congress on Milk Quality and Mastitis Control; 2000 Nov 13–16, Nagano, Japan; 2000. p. 547–52.
9. Takeishi M, Shimizu S, Tsumagari K, Kinoshita A, Yoshida S, Momotani E, et al. Studies on efficacy of the herbal MACH on IgE, interferon and intra-peritoneal macrophage in mice. In: Proceedings of the Fourth Advanced Traditional Chinese Veterinary Medicine Seminar; 2002 Oct 8–10, Guangzhou, China. Chi Institute, Florida, USA; 2002. p. 85–102.
10. Tarao K, Rino Y, Ohkawa S, Tamai S, Miyakawa K, Takekura H, et al. Close association between high serum alanine aminotransferase levels and multicentric hepatocarcinogenesis in patients with hepatitis C virus-associated cirrhosis. Cancer 2002;94:1787–95.
11. Moriya K, Fujie H, Shintani Y, Yotsuyanagi H, Tsutsumi T, Ishibashi K, et al. The core protein of hepatitis C virus induces hepatocellular carcinoma in transgenic mice. Nat Med 1998;4:1065–7.

Available online at www.sciencedirect.com

SCIENCE DIRECT

Genomics 84 (2004) 867–875

GENOMICS

www.elsevier.com/locate/ygeno

# Genome-wide transcriptome mapping analysis identifies organ-specific gene expression patterns along human chromosomes

Taro Yamashita[a], Masao Honda[a], Hajime Takatori[a], Ryuhei Nishino[a], Nobuaki Hoshino[b], Shuichi Kaneko[a,*]

[a]*Department of Cancer Gene Regulation, Kanazawa University Graduate School of Medical Science, 13-1 Takara-Machi, Kanazawa 920-8641, Japan*
[b]*Faculty of Economics, Kanazawa University, Kakuma-Machi, Kanazawa 920-1192, Japan*

Received 31 March 2004; accepted 6 August 2004
Available online 26 August 2004

**Abstract**

The Human Genome Project has revealed that there about 32,000 protein-encoding genes, which are distributed throughout the genome. It is unclear, however, whether genes are distributed on the chromosomes according to patterns linked to organ specificity. To explore the relationship between genes actively transcribed in normal tissues and their chromosomal locations, we analyzed serial analysis of gene expression libraries of normal human liver, brain, breast, and colon tissues. Transcriptome mapping analysis revealed that transcriptional activity in each tissue varied according to the chromosomal domains, and a weak positive correlation was observed between transcription density and gene density. We identified six liver-related and five colon-related chromosomal domains highly transcribed in each tissue, whereas no brain-related or breast-related chromosomal domains were identified. Representative genes located on these chromosomal domains were associated with the function of each organ and were highly conserved in both mouse and rat genomes. These data revealed that the transcriptional activities of normal human tissues are well orchestrated at chromosomal levels, suggesting that highly expressed genes may share physical proximity.


*Keywords:* Genomics; Gene expression profiling; Serial analysis of gene expression; Transcriptome mapping; Organ-related chromosomal domain

## Introduction

Analysis of the human genome has shown that there are about 32,000 protein-coding genes distributed throughout the 46 chromosomes. Previous work, however, indicated that the highly expressed genes in all human tissues are clustered in several chromosomal domains [1]. In the nematode *Caenorhabditis elegans*, genes expressed in the muscle are clustered in small groups along the chromosomes [2], suggesting a relationship between muscle-specific functionality and chromosomal domains actively transcribed in *C. elegans*. Another report revealed that groups of adjacent genes were coregulated in the fly *Drosophila melanogaster*, suggesting that coregulated genes also share physical proximity in *D. melanogaster* [3]. Furthermore, a comparative analysis of the genomes of *D. melanogaster*, *C. elegans*, and *Saccharomyces cerevisiae* revealed the existence of a "core proteome" highly conserved in yeast, worm, and fly [4], suggesting the heredity of fundamental genomic or proteomic organization associated with the cellular processes or functions commonly observed in all eukaryotes. From these reports, we postulated a hypothesis that the distribution of genes along human chromosomes may exhibit a higher level of organization, which may be linked to organ-specific functionality and conserved in mammals.

To explore the relationship between genes actively transcribed in normal human tissues and chromosomal domains, we analyzed serial analysis of gene expression (SAGE) libraries derived from normal human liver, brain,

* Corresponding author. Fax: +81 76 234 4250.
*E-mail address:* skaneko@medf.m.kanazawa-u.ac.jp (S. Kaneko).

0888-7543/$ - see front matter © 2004 Elsevier Inc. All rights reserved.
doi:10.1016/j.ygeno.2004.08.008

breast, and colon tissues with human genome sequence information. We observed organ-specific gene expression patterns along the chromosomes in each tissue, identifying six liver-related chromosomal domains and five colon-related chromosomal domains. We found that transcriptional activity in normal human tissues is well orchestrated at the chromosomal level, suggesting that most of the highly expressed genes in each organ might be clustered. We further observed that representative genes located on these chromosomal domains were associated with organ-specific function, and the genes were also clustered on the *Rattus norvegicus* and *Mus musculus* genomes. These findings may be the results of binding of specific transcription factors onto specific chromosomal domains in each tissue or of chromosome rearrangements during mammalian evolution.

## Results

### *Organ-specific gene expression patterns along the chromosome*

An outline of the construction of the transcriptome map is shown in Fig. 1. We assigned 27,402 NCBI RefSeq genes (build 31) to 17,193 Locus ID clusters. All SAGE tags detected could be assigned to a total of 55,612 reliable UniGene clusters using the SAGEmap reliable tag-to-gene mapping table (http://www.sagenet.org/SAGEDatabases/unigene.htm). All SAGE tags assigned were related to the Locus ID clusters by UniGene ID, and the origins of the start sites in all genes were mapped to the SAGE tag.

When we investigated the correlation between the number of genes and the number of transcripts in each chromosome using a 5-Mb window moving along the chromosome at 1-Mb intervals, we found that Pearson's correlation coefficients ranged from 0.119 to 0.869 in the liver, 0.107 to 0.838 in the brain, 0.314 to 0.791 in the breast, 0.206 to 0.872 in the colon, and 0.304 to 0.883 in the reference library (Table 1). These data suggested that the transcriptional activity in each tissue varied and was not in accordance with the number of genes encoded by each chromosome. The strongest positive correlations, however, were observed in the reference libraries, indicating that gene expression levels in total tissues could be relatively correlated with the number of genes per chromosome.

To investigate the transcription density along the human chromosomes using digital gene expression data, we calculated transcription density factor (TDF), which would be well correlated with the abundance of transcripts and adjusted by gene density in each chromosomal domain, as described under Materials and methods. When we calculated the gene density and TDF in each tissue on whole chromosomal domains, we found that gene expression levels fluctuated along the chromosome, with most genes in most chromosomal domains expressed at a range of $0.5 < TDF < 1.5$ in each tissue (representative transcriptome maps are shown in Fig. 2). Gene expression patterns in each of

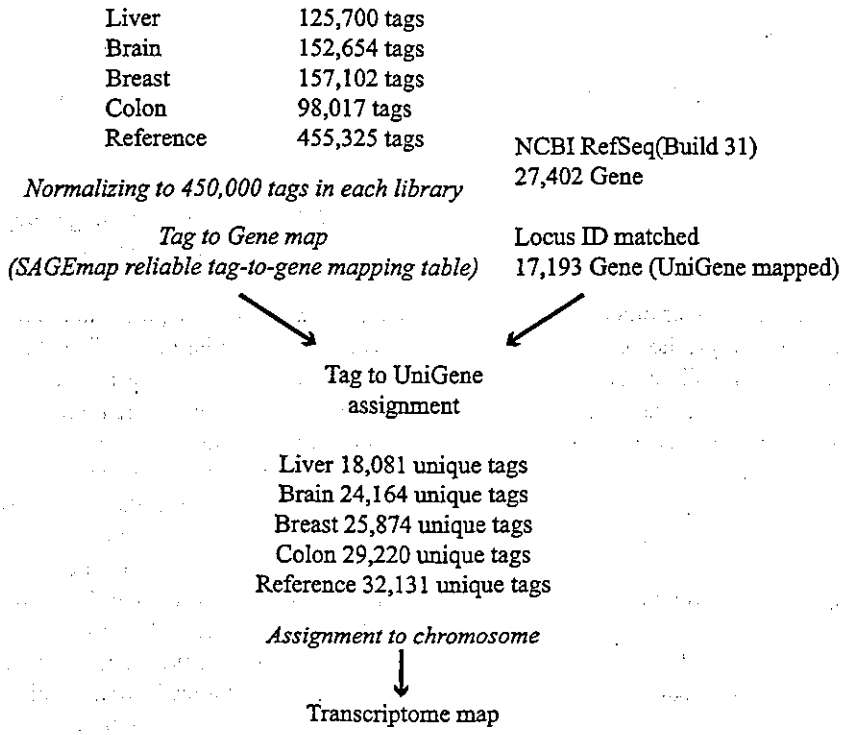


Fig. 1. Schematic outline of transcriptome map construction. All detected SAGE tags were assigned to a total of 55,612 reliable UniGene clusters and related to the Locus ID clusters by UniGene ID. Location of the SAGE tags on the chromosome was coordinated with physical distance information.

Table 1
Correlation between the number of transcripts and the number of genes in each chromosome

| Chromosome | Liver | Brain | Breast | Colon | Reference |
|---|---|---|---|---|---|
| 1 | 0.483 | 0.674 | 0.640 | 0.537 | 0.703 |
| 2 | 0.491 | 0.739 | 0.642 | 0.670 | 0.675 |
| 3 | 0.517 | 0.672 | 0.594 | 0.538 | 0.739 |
| 4 | 0.404 | 0.470 | 0.512 | 0.391 | 0.512 |
| 5 | 0.869 | 0.785 | 0.669 | 0.721 | 0.883 |
| 6 | 0.720 | 0.838 | 0.709 | 0.805 | 0.856 |
| 7 | 0.638 | 0.686 | 0.568 | 0.699 | 0.670 |
| 8 | 0.324 | 0.386 | 0.314 | 0.335 | 0.364 |
| 9 | 0.355 | 0.776 | 0.555 | 0.705 | 0.515 |
| 10 | 0.448 | 0.498 | 0.322 | 0.441 | 0.304 |
| 11 | 0.224 | 0.801 | 0.544 | 0.556 | 0.778 |
| 12 | 0.397 | 0.632 | 0.711 | 0.616 | 0.730 |
| 13 | 0.281 | 0.398 | 0.478 | 0.311 | 0.459 |
| 14 | 0.354 | 0.573 | 0.378 | 0.431 | 0.651 |
| 15 | 0.119 | 0.284 | 0.345 | 0.206 | 0.339 |
| 16 | 0.520 | 0.719 | 0.500 | 0.588 | 0.666 |
| 17 | 0.410 | 0.550 | 0.791 | 0.670 | 0.634 |
| 18 | 0.211 | 0.107 | 0.453 | 0.359 | 0.364 |
| 19 | 0.587 | 0.701 | 0.555 | 0.610 | 0.700 |
| 20 | 0.570 | 0.769 | 0.701 | 0.673 | 0.709 |
| 21 | 0.766 | 0.627 | 0.547 | 0.872 | 0.744 |
| 22 | 0.429 | 0.563 | 0.680 | 0.445 | 0.593 |
| X | 0.653 | 0.786 | 0.747 | 0.705 | 0.758 |
| Average | 0.468 | 0.610 | 0.563 | 0.560 | 0.624 |

these chromosomal domains were tissue specific, indicating the existence of distinct, organ-specific gene expression patterns along the chromosomes.

*Identification of organ-related chromosomal domains*

To determine whether each tissue type had distinct gene expression patterns along the chromosomes, we mathematically classified the chromosomal domains by TDF. For each tissue type, we determined if the TDF in a given SAGE library exceeded 1.8 and if the TDF in the other libraries was less than 1.0. The chromosomal domains identified by these criteria fulfilled the condition that gene expression levels in the given tissue were increased more than 6-fold compared with those of other tissues and that gene expression levels in the other tissues did not exceed the 2.7-fold of the reference levels. To diminish the effect of a gene highly expressed in a chromosomal domain of low gene density on a TDF score, we selected chromosomal domains more than 3 Mb long, containing more than two genes in a window of 1 Mb, with TDF >1.8 consecutively.

Using these criteria, we first compared the gene expression patterns of the liver. Using SAGE libraries derived from normal liver and a mixture of five normal livers, we investigated whether there were individual variations in hepatic gene expression patterns along the chromosome. The TDF derived from the normal liver SAGE library could be correlated with the TDF derived from the mixture of five normal liver SAGE libraries, with Pearson's correlation coefficient ranging from 0.618 to 0.960. In addition, the difference between the TDF in the normal liver library and that in the pooled liver library never exceeded 1.8 on all chromosomal domains (data not shown), indicating that there were no individual differences of more than sixfold along the chromosome. These data also suggested that the criteria used here could enable us to disregard the individual variations in gene expression patterns and could be useful for identifying chromosomal domains actively transcribed in each tissue type.

We investigated whether highly expressed genes clustered along the chromosome in each tissue and applied the criteria to the mapping data of the liver, brain, breast, and colon SAGE libraries. After filtering transcriptome mapping data of the liver, we found that genes highly expressed in the liver were clustered in six chromosomal domains, compared with the brain, breast, and colon libraries. Similarly, we identified five colon-related chromosomal domains, but no brain-related or breast-related chromosomal domains.

To rule out the possibility of chance observation of high variance in the selected domains, we performed a permutation test as described under Materials and methods. The identified liver-related chromosomal domains and colon-related chromosomal domains were fully significant (liver-related chromosomal domains $p < 0.0001$, colon-related chromosomal domains $p < 0.0001$), revealing the statistical validity of our criteria.

Representative transcriptome mapping data and chromosomal domains are shown in Fig. 2 (chromosomes 1 and 6). Cytogenetically, we found liver-related chromosomal domains at 1q23–q25, 4q21–q24, 6p12.1, 11q23–q24, 17q11, and 18q12; we found colon-related chromosomal domains at 2p21, 3q23, 8q21, 12q15, and 21q22.

The numbers of SAGE tags distributed in each organ-related chromosomal domain are shown in Table 2. In liver-related chromosomal domains, the average gene expression levels in the liver were increased 18.1-, 22.2-, and 22.5-fold compared with levels in the brain, breast, and colon, respectively. In colon-related chromosomal domains, the average gene expression levels in the colon were increased 15.0-, 13.3-, and 8.0-fold compared with levels in the liver, brain, and breast, respectively.

*Conservation of the organ-related chromosomal domains in human and rodent genomes*

To examine whether organ-related chromosomal domains were preserved in other mammalian genomes, we investigated the possible homologous genes and their locations on the *R. norvegicus* and *M. musculus* genomes using the HomoloGene database. Of 412 human genes comprising 11 organ-related chromosomal domains, we identified 213 rat homologous genes (51.7%) and 230 mouse homologous genes (55.8%). Almost all of the homologous genes on human chromosomes 1q23–q25, 2p21, 3q23, 4q21–q24, 11q23, 12q15, 17q11, 18q12.1, and Xq21.3–q22 were located on the same chromosomal

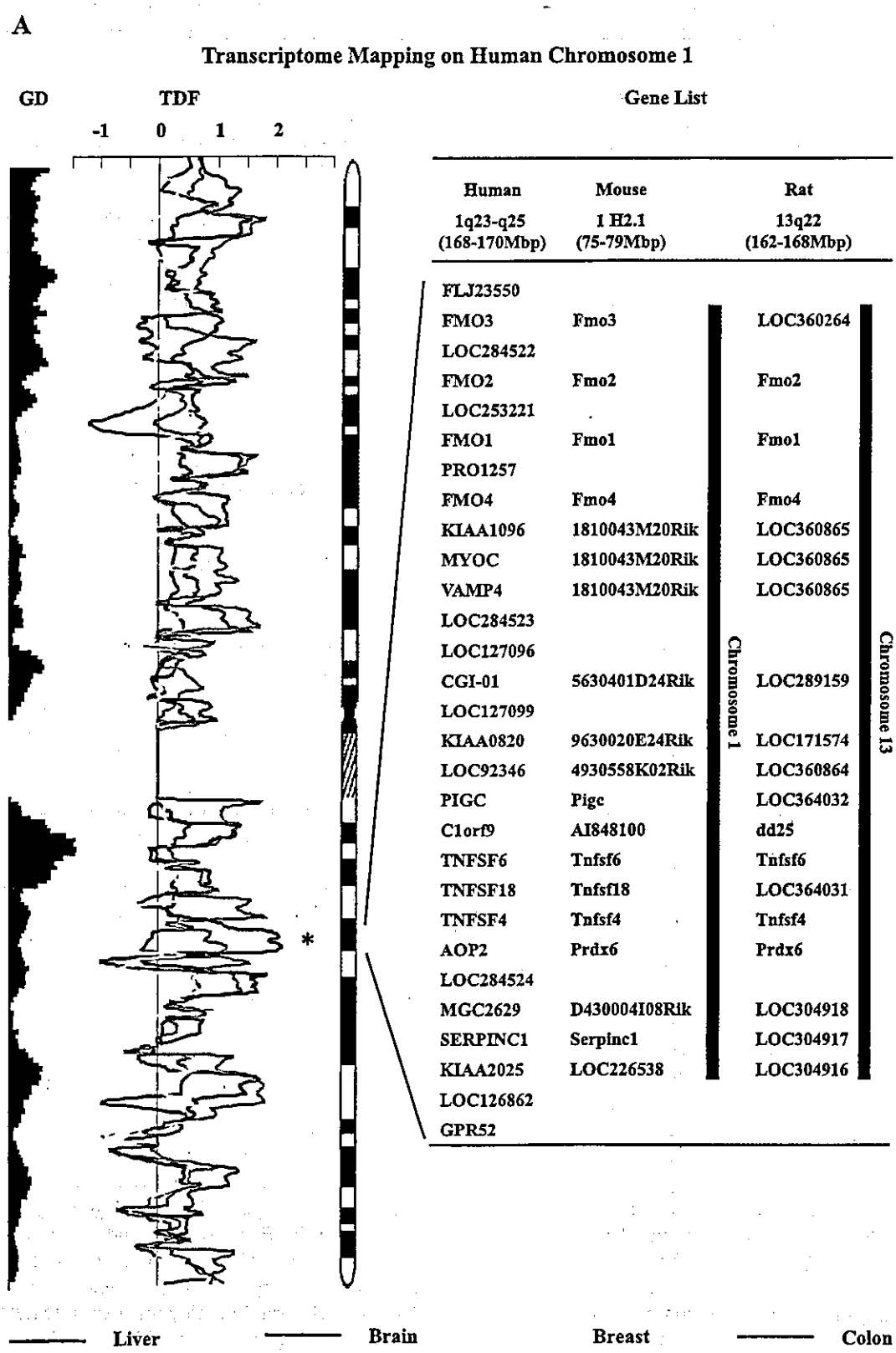


Fig. 2. Representative transcriptome map analysis of liver, brain, breast, and colon SAGE libraries. Differential expression patterns were observed in each tissue along the chromosome, and asterisks indicate the organ-related chromosomal domain. The genes located on the organ-related chromosomal domain in human are shown. Their possible homologous genes on mouse and rat genome are also shown.

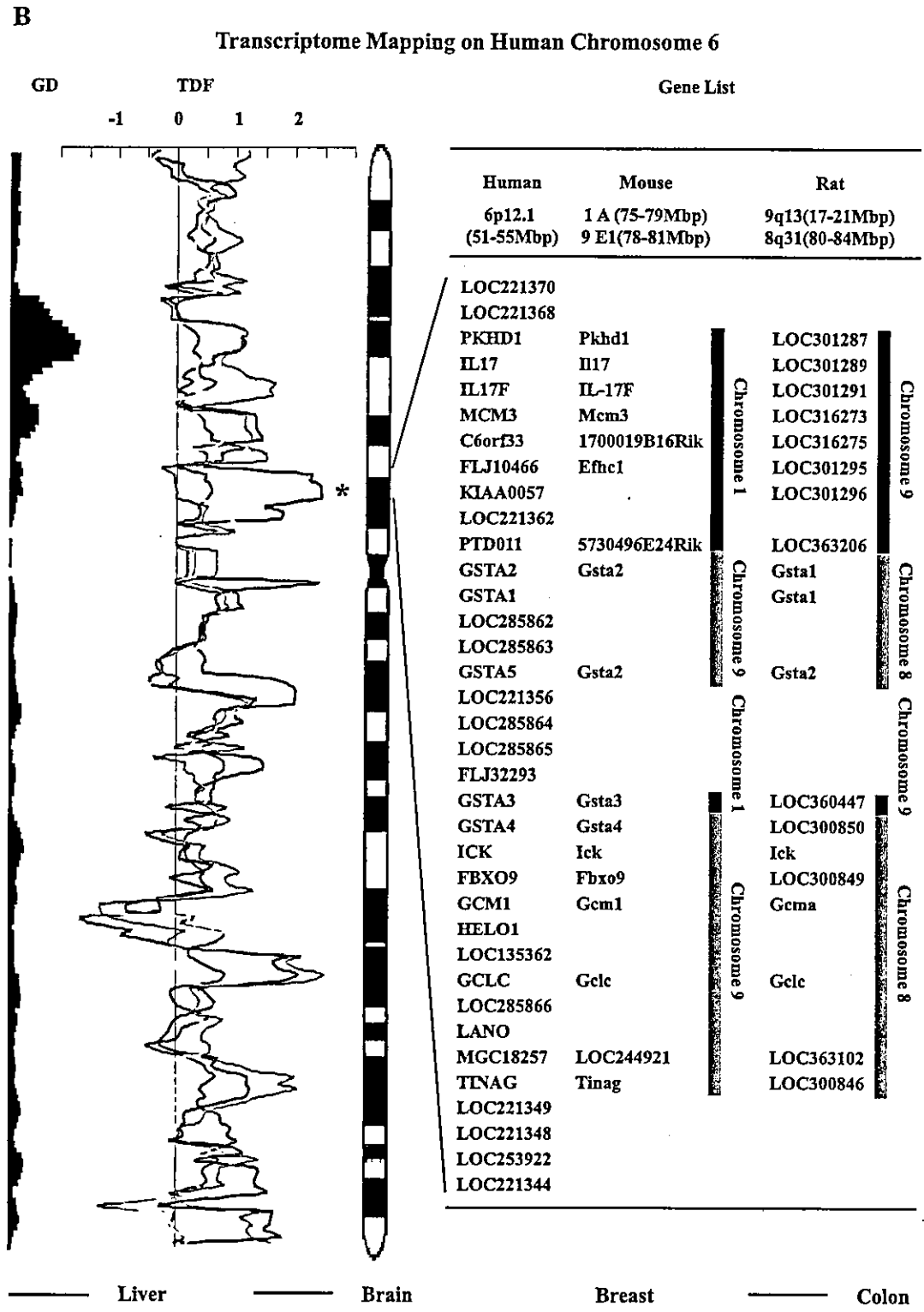


Fig. 2 (*continued*).

domains of the mouse and rat genomes (representative data of human 1q23–q25, mouse 1H2.1, and rat 13q22 are shown in Fig. 2). However, genes on chromosomes 6p12.1 and 21q22 were located on two different chromosomal domains of the rat and mouse genomes (representative data of human 6p12.1, mouse 1A and 9E1, and rat 9q13 and 8q31 are shown in Fig. 2). Interestingly, more than half of these chromosomal domains (1q23–q25, 4q21–q24, 6p12.1, 11q23, 18q12.1, and 21q22) contained multigene families. These data revealed that most of organ-related chromosomal domains identified here are conserved in the human and rodent genomes, which might have originated from chro-

Table 2
Cytogenetic loci of gene clusters highly expressed in each organ

| Cytogenetic locus | Liver | Brain | Breast | Colon | Reference |
|---|---|---|---|---|---|
| *Liver-related chromosomal domains* | | | | | |
| 1q23–q25 | 1,326 | 140 | 169 | 326 | 370 |
| 4q21–q25 | 2,104 | 132 | 139 | 129 | 352 |
| 6p12.1 | 983 | 189 | 166 | 84 | 210 |
| 11q23.1–q23.2 | 30,168 | 932 | 840 | 804 | 3552 |
| 17q11 | 3,329 | 777 | 445 | 385 | 778 |
| 18q12.1 | 1,752 | 26 | 26 | 28 | 168 |
| Total | 39,662 | 2196 | 1785 | 1756 | 5430 |
| *Colon-related chromosomal domains* | | | | | |
| 2p21 | 40 | 72 | 127 | 411 | 154 |
| 3q22–q23 | 59 | 55 | 86 | 406 | 116 |
| 8q13–q22.1 | 62 | 32 | 49 | 531 | 139 |
| 12q14.1–q21.1 | 35 | 37 | 53 | 510 | 132 |
| 21q22.3 | 25 | 52 | 100 | 1447 | 265 |
| Total | 221 | 248 | 415 | 3305 | 806 |

mosomal rearrangement and/or gene duplication during mammalian evolution (supplementary figure of all transcriptome mapping data and the gene list are available on our home page: http://www.intmedkanazawa.jp/).

### *Analysis of gene function on organ-related chromosomal domains*

We investigated the functions of genes clustered on organ-related chromosomal domains using the Gene Ontology database (http://www.geneontology.org/). We could retrieve the information for 227 of 412 clustered genes from the Gene Ontology database, and 150 of these were annotated by molecular function. Interestingly, 74 of 150 genes were associated with metabolic enzymes, revealing that about half of the genes clustered on organ-related chromosomal domains are those encoding metabolic enzymes, suggesting the close relation of the chromosomal domains and some metabolic processes.

We searched the downstream targets of the genes on the organ-related chromosomal domains using PathwayAssist software and investigated the common targets and functions of the genes on the chromosomal domains. As shown in Table 3, 10 of 11 organ-related chromosomal domains consisted of genes associated with common metabolic or functional pathways, whereas no common targets were detected on chromosome 12q15 (colon-related chromosomal domain). Apparently, gene families associated with metabolism are clustered in liver-related chromosomal domains, such as 6p12.1 with xenobiotic metabolism, 4q21–q24 with alcohol and aldehyde metabolism, and 11q23–q24 with lipid metabolism. On the other hand, genes associated with transporters and apoptosis were clustered in colon-related chromosomal domains, such as 8q21 with anion transporter and 21q22 with apoptosis and cell proliferation. These data suggested that the genes clustered on organ-related chromosomal domains might be associated with the organ-specific functionality.

## Discussion

The release of the sequence of the entire human genome and the development of advanced gene expression profiling technologies have focused interest on understanding the relationship between gene expression and chromosomal organization in complex systems. The genome is not simply a patchwork of genes but forms complex structures. The presence of chromosomal regions enriched in gene families has been demonstrated for several gene clusters. For example, the major histocompatibility complex is located on chromosome 6p21 [5], and the apolipoproteins are located on chromosome 11q23 [6]. It is not known, however, if genes abundantly expressed in each organ are distributed throughout the genome or clustered on various chromosomes. This question was addressed by assessing the chromosomal distribution of genes expressed in the brain and heart using EST collection databases [7,8]. Although these studies reported complex tissue-specific gene regulation patterns in the brain and heart, organ-specific gene expression patterns have not been compared simultaneously in several tissues. In addition, since EST databases are not generated according to the same methods by each distributor, comparison of the expression levels between organs may not be accurate. In this study, therefore, we utilized SAGE analysis to obtain unbiased gene expression data from hundreds of thousands of transcripts expressed in the normal human liver, brain, breast, and colon. Using genome-wide transcriptome maps for each organ, we identified six liver-related and five colon-related chromosomal domains. Thus, it seemed that organ-specific genes are accumulated on specific chromosomal domains for each organ.

Table 3
Functional annotation of the genes located on organ-related chromosomal domains

| Cytogenetic locus | Function |
|---|---|
| *Liver-related chromosomal domains* | |
| 1q23–q25 | Xenobiotic mono-oxygenation; apoptosis and cell proliferation |
| 4q21–q25 | Alcohol and formaldehyde metabolism |
| 6p12.1 | Xenobiotic metabolism |
| 11q23.1–q23.2 | Lipid metabolism |
| 17q11 | Amyloid production |
| 18q12.1 | Focal contact; apoptosis and cell proliferation |
| *Colon-related chromosomal domains* | |
| 2p21 | Apoptosis and cell proliferation |
| 3q22–q23 | Ion transporter; apoptosis and cell proliferation |
| 8q13–q22.1 | Ion transporter; apoptosis and cell cycle regulation |
| 12q14.1–q21.1 | None |
| 21q22.3 | Apoptosis and cell proliferation; mucin production |

Although the biological significance of this clustering of highly expressed, organ-related genes along the chromosomes is not clear, these clusters must provide significant advantages for tissue-specific functioning. The functional annotation of liver-related chromosomal domains revealed that they encoded metabolism-related genes such as for xenobiotic, lipid, and alcohol metabolism. The lipid and alcohol metabolism is liver specific. The functional annotation of colon-related chromosomal domains revealed that they encoded apoptosis, cell proliferation, ion transporter, and mucin production. These functions are essential for colon epithelium producing gut fluid and compatible with the short life span of the colon epithelium [9,10]. Thus, we first identified the presence of organ-related gene clusters in chromosomes and revealed their biological significance for organ-specific functioning.

In general, the relative proportions of cell types differ in each organ and affect the patterns of gene expression. In this study, we identified six liver-related and five colon-related chromosomal domains, whereas no brain-related or breast-related chromosomal domains were found on whole chromosome. It is possible that different compositions of cells might underestimate the presence of organ-related gene clusters in chromosomes.

What is the biological and evolutionary background of these organ-related chromosomal domains? In general, transcriptional machineries may access two coexpressed genes more efficiently when they are neighbors, so active transcription of organ-related chromosomal domains may result from the binding of a specific transcription factor to these domains [2]. Another possibility is that the formation of organ-related chromosomal domains in the human genome is the result of chromosome rearrangement during the process of evolution, because the organ-related chromosomal domains were conserved in one or two mouse and rat chromosomes. Recent comparative analyses of large-scale genome sequencing revealed that rearrangement of chromosomal segments and localized duplication of genomic segments are two major factors in eukaryotic genome evolution [11]. Our data revealed that half of the organ-related chromosomal domains contained multigene families. These results suggest that the gene duplications may also contribute to the formation of organ-specific functionality in mammalian evolution.

Recently, draft genome sequences of the Brown Norway rat were analyzed and compared with the human and mouse genomes, revealing that the human and rodent genomes contain conserved synteny blocks [12]. We therefore investigated the organ-related chromosomal domains with reported conserved synteny blocks in human, mouse, and rat genomes (http://www.genboree.org) and identified that all organ-related chromosomal domains were included in synteny blocks conserved in human and rodent genomes (data not shown). These data might indicate the proximity of the human and rodent genomes in mammalian evolution, and organ-related chromosomal domains may have constituted parts of synteny blocks of larger size during human, mouse, and rat genome evolution.

If the number of genes in a chromosomal domain were small and the transcriptional activity in most of a tissue were low in the 5-Mb window, we could not eliminate the effects of a single highly expressed gene on the TDF score. To eliminate this limitation, we set the region criteria of gene density to more than two genes in a window of 1 Mb. Another limitation of the method is the inability to reveal some chromosomal domains with equal up–down differential gene expression. Although the method in this study still has some limitations, our data could provide the candidate organ-related chromosomal domains and could highlight the neighboring genes on the domains with tissue specificity.

In conclusion, we have identified gene expression patterns along the chromosomes in normal human liver, brain, breast, and colon, showing the clustering of organ-related genes on specific chromosomal domains. Our results indicate that the human genome organization may be closely related to the organ-specific gene expression patterns.

## Materials and methods

### *SAGE*

To determine organ-specific gene expression patterns comprehensively along human chromosomes, we collected SAGE databases derived from normal tissues. To avoid individual variations in gene expression, we selected, for each tissue, SAGE libraries that contained at least 50,000 tags, and we used at least two libraries per tissue type. We analyzed publicly available SAGE libraries derived from normal brain (GSM676, GSM695), breast (GSM677, GSM780, GSM781), and colon (GSM728, GSM729) tissues (ftp://ftp.ncbi.nih.gov/pub/sage/). We also constructed SAGE libraries derived from normal liver tissues (http://www.intmedkanazawa.jp/) [13], as well as reference SAGE databases containing publicly available normal human brain, breast, colon, heart, kidney, liver, lung, prostate, and stomach SAGE libraries (GSM761, GSM677, GSM728, GSM1499, GSM708, GSM785, GSM762, GSM739, GSM739, and GSM784), each containing about 50,000 SAGE tags. All sequence files from these databases were analyzed with SAGE 2000 software, kindly donated by Drs. Kenneth W. Kinzler and Bert Vogelstein. The number of SAGE tags per library was normalized to 450,000 transcripts.

### *Transcriptome mapping*

Gene identity and UniGene CLUSTER assignment of each SAGE tag were obtained from the SAGEmap reliable tag-to-gene mapping table (http://www.sagenet.org/SAGEDatabases/unigene.htm). Association of UniGene

clusters with chromosome positions was obtained from RefSeq build 31 (http://www.ncbi.nlm.nih.gov/RefSeq/) and LocusLink (http://www.ncbi.nlm.nih.gov/LocusLink/) databases (November 26, 2002). SAGE tag locations along the chromosomes were matched to physical distance information by connecting the SAGE map, RefSeq, and LocusLink tables with the UniGene number.

*Transcription density and gene density*

Transcriptional activity was determined from the TDF [7]. Briefly, TDF is calculated using a 5-Mb window moving along the chromosome at 1-Mb intervals and defined as TDF = $\ln(R/R_{\mathrm{ref}})/(T/T_{\mathrm{ref}})$, where $R$ is the number of SAGE tags in each library and $T$ is the number of unique SAGE tags in each library, within a window of 5 Mb. Gene density is defined as the number of RefSeq records divided by the average RefSeq records in each 5-Mb window. The correlation between transcription density and gene density in each chromosome was assessed by calculating the Pearson's correlation coefficient using the equation

$$r=\frac{n\left(\sum_{i=1}^{n} XiYi\right)-\left(\sum_{i=1}^{n} Xi\right)\left(\sum_{i=1}^{n} Yi\right)}{\sqrt{\left\{n\sum_{i=1}^{n} Xi^2-\left(\sum_{i=1}^{n} Xi\right)^2\right\}\left\{n\sum_{i=1}^{n} Yi^2-\left(\sum_{i=1}^{n} Yi\right)^2\right\}}}$$

where $X_i$ is the number of SAGE tags in each library and $Y_i$ is the number of RefSeq records in each 5-Mb window.

To investigate the statistical significance of the TDF values selected, we performed a permutation test. The following argument explains a statistical method that tests the null hypothesis that two groups are equivalent in the distribution of orders of their members. The alternative hypothesis is that members of one of the groups tend to rank higher. By rejecting the null hypothesis, we show that selected members are significantly high-ranked in the order of a variable. First we set up the notation. Suppose that $n$ regions are classified into two groups. Each region is indexed by $i$, where $i \in I = \{1,2,\ldots,n\}$ and $I_1$ denotes the set of indices of the first group of $m$ regions. Assuming that an observed value $x_i$ is attributed to the $i$th region, we denote the order statistics of the values by $x_{(1)} > x_{(2)} > \ldots > x_{(n)}$, where no tie is assumed to simplify the argument. Let a function $\rho(i)$, $i \in I$ uniquely assign to an index its rank: $x_i = x_{(\rho(i))}$.

A permutation test is adopted, and without loss of generality, we henceforth assume that $I_1 = \{1, 2, \ldots, m\}$. Under the null hypothesis,

$$Pr(\rho(1)) = i_1, \rho(2) = i_2,\ldots, \rho(m) = i_m) = \frac{1}{\binom{n}{m}}$$

for all the elements of $\{(i_1,i_2,..i_m)\in I^m \mid \forall j\neq k, i_j\neq i_k, (j,k)\in I_1^2\}$.

Let us consider the test statistic $T = \sum_{i=1}^{m} \rho(i)$ where the null hypothesis is rejected for some $c$ if $T < c$. Consequently, the $p$ value of a realized test statistic $t$ is given by $Pr(T \leq t)$. In particular, if the regions of the first group are ranked from the first to the $m$th, the $p$ value reduces to

$$Pr\left(T \leq \frac{m(1+m)}{2}\right) = \frac{1}{\binom{n}{m}}$$

To be concrete, let us regard $x_i$ as the TDF of the $i$th region, for example. Top $m$ ranks group together under the criterion that selects the regions where TDFs are larger than 1.8. Hence its significance is easy to evaluate by the aforesaid method, and the rejection of the null hypothesis implies that the selected regions' TDFs are larger. Similarly, if we select the regions where an objective organ's TDF is larger than 1.8 and other organs' TDFs are smaller than 1.0, just regard $x_i$ as the number of organs whose TDFs are smaller than 1.0. Then top $m$ ranks consist of the selected regions among $n$ regions where an objective organ's TDF is larger than 1.8. In this case, the rejection of the null hypothesis implies that the TDFs of organs other than the objective are relatively small in the selected regions.

*Comparison of organ-related chromosomal domains in rat, mouse, and human genomes*

All genes located on organ-related chromosomal domains in human were listed using the RefSeq build 31 database (http://www.ncbi.nlm.nih.gov/RefSeq/). All possible homologous genes and their locations on the *R. norvegicus* and *M. musculus* genomes were searched using the HomoloGene database (February 20, 2004) (http://www.ncbi.nlm.nih.gov/entrez/query.fcgi?DB=homologene). The chromosomal location and the gene list on each domain were also confirmed by MapViewer (http://www.ncbi.nlm.nih.gov/mapview/).

*Pathway analysis*

To investigate the functions of genes located on organ-related chromosomal domains comprehensively, we used PathwayAssist software (Ariadone Genomics, Rockville, MD, USA). All genes located on the chromosomal domains were investigated and annotated with the biological processes, protein–protein interactions, and gene regulatory networks using a reference-based data file.

**Acknowledgment**

The authors thank Dr. Koichi Miwa for providing human liver tissues.

## References


[1] H. Caron, et al., The human transcriptome map: clustering of highly expressed genes in chromosomal domains, Science 291 (2001) 1289–1292.

[2] P.J. Roy, J.M. Stuart, J. Lund, S.K. Kim, Chromosomal clustering of muscle-expressed genes in Caenorhabditis elegans, Nature 418 (2002) 975–979.

[3] P.T. Spellman, G.M. Rubin, Evidence for large domains of similarly expressed genes in the Drosophila genome, J. Biol. 1 (2002) 5.

[4] G.M. Rubin, et al., Comparative genomics of the eukaryotes, Science 287 (2000) 2204–2215.

[5] H. Abderrahim, et al., Cloning the human major histocompatibility complex in YACs, Genomics 23 (1994) 520–527.

[6] K. Omori, L. Vergnes, M.M. Zakin, A. Ochoa, The apolipoprotein AICIII–AIV gene cluster: sequence of the ApoCIII–ApoAIV intergenic region, Gene 159 (1995) 231–234.

[7] P. Qiu, L. Benbow, S. Liu, J.R. Greene, L. Wang, Analysis of a human brain transcriptome map, BMC Genom. 3 (2002) 10.

[8] J.D. Barrans, et al., Chromosomal distribution of the human cardiovascular transcriptome, Genomics 81 (2003) 519–524.

[9] K. Kunzelmann, M. Mall, Electrolyte transport in the mammalian colon: mechanisms and implications for disease, Physiol. Rev. 82 (2002) 245–289.

[10] P. de Santa Barbara, G.R. van den Brink, D.J. Roberts, Development and differentiation of the intestinal epithelium, Cell. Mol. Life Sci. 60 (2003) 1322–1332.

[11] E.E. Eichler, D. Sankoff, Structural dynamics of eukaryotic chromosome evolution, Science 301 (2003) 793–797.

[12] R.A. Gibbs, et al., Genome sequence of the Brown Norway rat yields insights into mammalian evolution, Nature 428 (2004) 493–521.

[13] T. Yamashita, et al., Comprehensive gene expression profile of a normal human liver, Biochem. Biophys. Res. Commun. 269 (2000) 110–116.

[CANCER RESEARCH 64, 3326–3333, May 1, 2004]



# Different Procarcinogenic Potentials of Lymphocyte Subsets in a Transgenic Mouse Model of Chronic Hepatitis B

Yasunari Nakamoto,[1] Takashi Suda,[2] Takashi Momoi,[3] and Shuichi Kaneko[1]

[1]Department of Gastroenterology, Graduate School of Medicine, [2]Center for the Development of Molecular Target Drugs, Cancer Research Institute, Kanazawa University, Kanazawa, and [3]Division of Development and Differentiation, National Institute of Neuroscience, NCNP, Kodaira, Tokyo, Japan

## ABSTRACT

**The immune response to hepatitis viruses is believed to be involved in the development of chronic hepatitis; however, its pathogenetic potential has not been clearly defined. The current study, using a transgenic mouse model of chronic hepatitis B, was designed to determine the relative contributions of the immune cell subsets to the progression of liver disease that induces hepatocellular carcinogenesis. Hepatitis B virus transgenic mice were adoptively transferred with $CD4^+$ and $CD8^+$ T cell-enriched or -depleted and B cell-depleted splenocytes obtained from hepatitis B surface antigen-primed, syngeneic nontransgenic donors. The resultant liver disease, hepatocyte apoptosis, regeneration, and tumor development were assessed and compared with the manifestations in mice that had received unfractionated spleen cells. Transfer of $CD8^+$-enriched splenocytes caused prolonged disease kinetics, and a marked increase in the extent of hepatocyte apoptosis and regeneration. In 12 of 14 mice the transfer resulted in multiple hepatocellular carcinomas (HCCs) comparable with the manifestations seen in the mice transferred with total splenocytes. In contrast, mice that had received $CD4^+$-enriched cells demonstrated lower levels of liver disease and developed fewer incidences of HCC (4 of 17). The experiment also revealed that all of the groups of mice complicated with HCC developed comparable mean numbers and sizes of tumors. B-cell depletion had no effect on disease kinetics in this model. Taken together, these results demonstrate that the pathogenetic events induced by $CD8^+$ T-cell subset are primarily responsible for the induction of chronic liver disease that increases tumor incidence, suggesting their potential in triggering the process of hepatocarcinogenesis.**

## INTRODUCTION

Hepatocellular carcinoma (HCC) occurs after many years of chronic hepatitis (1, 2). During the process, both viral and host factors have been implicated in liver cell transformation and carcinogenesis. On the one hand, some viral proteins, *i.e.*, hepatitis B virus (HBV) X protein (3, 4) and hepatitis C virus core protein (5, 6), are considered to contribute to tumor development in the liver, because high-level expression of the proteins increases the incidence of HCC in transgenic mice. Furthermore, most tumors contain clonally integrated HBV DNA and microdeletions in the flanking cellular DNA, which could theoretically deregulate cellular growth control mechanisms (7). And COOH-terminally truncated viral envelop proteins expressed from integrated subviral DNA may have transactivating activity (8, 9) and could potentially contribute to carcinogenesis in chronic HBV infection.

On the other hand, prolonged inflammation is thought to set up a cycle of liver cell destruction and regeneration, resulting in a mitogenic and mutagenic environment that can precipitate random genetic and chromosomal damage, and lead to the development of HCC (10–12). In patients with chronic hepatitis B and C, $CD4^+$ and $CD8^+$ T lymphocytes specific for the viruses are detectable in the peripheral blood and in intrahepatic infiltrates, and are suggested to play a role in the immune pathogenesis of liver disease (13–16). Furthermore, transfer of the virus-specific $CD4^+$ and $CD8^+$ T-cell clones was observed to induce acute necroinflammatory liver disease in the models of HBV transgenic mice (17–20). However, the relative contribution of $CD4^+$ and $CD8^+$ T lymphocytes to the induction of chronic liver cell injury was not determined, because the T-cell clones induced neither prolonged liver diseases nor HCC in the models of acute hepatocellular injury, and because the animal model that pathophysiologically reproduces human chronic viral hepatitis was not available. In an effort to clarify the carcinogenic potential of chronic inflammation, we have developed a model of chronic immune-mediated liver disease using HBV transgenic mice that express the envelop proteins in the hepatocytes (21). The results demonstrate that continuous intrahepatic inflammation is sufficient to cause liver cancer in the absence of pre-existing viral transactivation, insertional mutagenesis, or genotoxic chemicals during chronic HBV infection.

We have shown recently that the administration of anti-Fas ligand (FasL) neutralizing antibody reduces hepatocyte apoptosis, proliferation, and liver inflammation, and eventually diminishes the development of HCC. This observation suggests a critical involvement of FasL-induced pathogenetic events in the process of hepatocarcinogenesis (22). We have also reported evidence that the FasL-dependent pathway is critically involved in the development of acute liver cell injury induced by $CD8^+$ cytotoxic T-lymphocyte (CTL) clones (23, 24). Because FasL is known to be expressed on activated T lymphocytes (25–29), we speculated that the $CD8^+$ T-cell subset was implicated as a causative factor responsible for the chronic liver cell injury that promotes hepatocarcinogenesis.

To determine the involvement of immune cell subsets in the progression of chronic liver disease, the current experiment was performed in the model of chronic immune-mediated hepatitis in which T- and B-cell subset-depleted or -enriched splenocytes obtained from HBV-primed, nontransgenic mice were transferred into the transgenic recipients, and liver disease and tumor development were monitored. The results demonstrate that each cell subset causes unique kinetics of liver disease and different incidence of liver cancer.

## MATERIALS AND METHODS

**HBV Transgenic Mice.** Hepatitis B surface antigen (HBsAg) transgenic mouse lineage 107–5D [official designation Tg(Alb-1, HBV)Bri66; inbred B10D2, H-$2^d$ ] was kindly provided by Dr. Francis V. Chisari (The Scripps Research Institute, La Jolla, CA; Ref. 30). Lineage 107–5D contains the entire HBV envelope coding region (subtype ayw) under the constitutive transcriptional control of the mouse albumin promoter (30). These mice express the HBV small, middle, and large envelope proteins in their hepatocytes (30, 31), they are immunologically tolerant to HBsAg at the T-cell level (32), and they display no evidence of liver disease during their lifetime although they do develop "ground glass" hepatocytes due to overexpression of the large envelope protein (30). There is no X-RNA or X-protein expression detectable in the livers of these animals.[4] Importantly, the mice develop a severe MHC class I-restricted necroinflammatory liver disease after the adoptive transfer of HBsAg-specific CTLs (17, 18, 30).

Received 12/6/03; revised 2/5/04; accepted 2/25/04.

The costs of publication of this article were defrayed in part by the payment of page charges. This article must therefore be hereby marked *advertisement* in accordance with 18 U.S.C. Section 1734 solely to indicate this fact.

Requests for reprints: Shuichi Kaneko, Department of Gastroenterology; Graduate School of Medicine, Kanazawa University; 13-1 Takara-machi, Kanazawa 920-8641, Japan. Phone: 81-76-265-2231; Fax: 81-76-234-4250; E-mail: skaneko@medf.m.kanazawa-u.ac.jp.

[4] Unpublished observations.

**Disease Model.** To break tolerance at the B- and T-cell levels, HBV transgenic mice were thymectomized, bone marrow-reconstituted, and adoptively transferred with nontransgenic immune systems according to the procedures described previously (21, 33). Briefly, 8–10-week-old male transgenic mice were thymectomized. Seven days later the mice were irradiated (900 cGy) and then reconstituted by the i.v. injection of $10^7$ bone marrow cells collected from the femurs and tibias of syngeneic nontransgenic B10D2 (H-$2^d$) mice. One week after the bone marrow transfer, the animals were injected i.v. with the indicated numbers of splenocyte subsets from nontransgenic B10D2 (H-$2^d$) mice that were infected i.p. with a recombinant vaccinia virus expressing HBsAg (HBs-vac) 3 weeks before the splenocyte transfer (17). At the same time, transfer of total splenocytes from the primed nontransgenic mice and the unprimed transgenic littermates were performed for control purposes. The resultant hepatocellular injury was monitored biochemically as serum alanine aminotransferase (ALT) activity (10). Results were expressed as mean units per liter ± SE of serum ALT activity, and differences between groups were assessed for statistical significance by Student's *t* test. Tumor development was assessed by abdominal palpation and confirmed by autopsy at which time the number of tumors visible at the surface of each liver was counted, and the diameter of each tumor was measured with a millimeter rule. All of the experiments satisfied the Guidelines for the Care and Use of Laboratory Animals in Takara-machi Campus of Kanazawa University.

**Depletion and Enrichment of T- and B-Cell Subsets.** To deplete $CD4^+$ or $CD8^+$ T cells, splenocytes were treated with monoclonal antibodies (mAbs) specific for CD4 (GK1.5) or CD8 (2.43; American Type Culture Collection, Manassas, VA), respectively, and then with rabbit complement (Cedarlane, Hornby, Ontario, Canada). B cells of splenocytes were depleted on the Mouse T Cell immunocolumn (Cytovax, Edmonton, Alberta, Canada), by treatment with mAb specific for MHC class II I-$A^d$ (MK-D6; American Type Culture Collection), and with rabbit complement. To enrich $CD4^+$ or $CD8^+$ T cells, splenocytes were passed over the Mouse T Cell immunocolumn and treated with a combination of anti-CD8 and anti-I-$A^d$ mAbs, or anti-CD4 and anti-I-$A^d$ mAbs, respectively, and then with rabbit complement. The purity of the T- and B-cell populations was monitored by immunolabeling with FITC-conjugated rat mAb specific for mouse CD4 (RM4–5; BD PharMingen, San Diego, CA), and phycoerythrin-conjugated rat mAb specific for mouse CD8 (53–6.7), or CD19, which is a B cell-specific transmembrane protein (1D3; BD PharMingen), followed by fluorescence-activated cell sorter analysis.

**Immunohistochemical Analysis.** Tissue samples were fixed in buffered zinc formalin (Anatech Ltd., Battle Creek, MI), embedded in paraffin, sectioned (at 3 $\mu$ m), and stained with H&E as described previously (21). Some of the paraffin sections were treated with anti-proliferating cell nuclear antigen (PCNA) and anti-HBsAg primary solutions (Dako, Carpinteria, CA) at 1:10 and 1:1000 dilutions, respectively, followed by biotin-conjugated secondary antibody (Vector Laboratories, Inc., Burlingame, CA; Ref. 34). $PCNA^+$ and $HBsAg^+$ cells were then visualized using a VECTASTAIN ABC Standard kit (Vector Laboratories), and the tissue sections were counterstained with hematoxylin before mounting. Liver tissue samples were also embedded in OCT compound (Sakura Finetek, Torrance, CA) and snap-frozen in liquid nitrogen. Cryostat sections of frozen tissues were fixed in 4% paraformaldehyde overnight at 4°C. After blocking biotin, the tissue sections were incubated with rabbit antimouse active caspase-3 antibodies (35) at a 1:400 dilution for 30 min at room temperature, followed by biotin-conjugated goat antirabbit IgG secondary antibodies (Vector Laboratories). The reaction was visualized in the same way as the PCNA staining described above. Terminal deoxynucleotidyl transferase-mediated nick end labeling (TUNEL) analysis was performed on serial liver sections according to the manufacturer's instructions (Roche, Indianapolis, IN).

## RESULTS

**Cellular Basis for Prolonged Chronic Immune-Mediated Hepatitis in HBV Transgenic Mice.** To determine the relative contribution of immune cell subsets to prolonged chronic immune-mediated hepatitis in HBV transgenic mice, the splenocytes isolated from HBsAg-primed nontransgenic mice were depleted (Fig. 1) or enriched (Fig. 2) of $CD4^+$ and $CD8^+$ T cells and $CD19^+$ B cells, and they were then adoptively transferred into thymectomized, bone marrow-reconstituted HBV transgenic recipients. The kinetics of all of the disease manifestations was compared with that caused by total splenocyte transfer. As observed previously (21), total cell transfer caused prolonged chronic hepatitis (Fig. 1). Briefly, serum ALT activity increased from preinjection levels of 20–40 units/liter to approximately 2000–4000 units/liter within 7 days after adoptive transfer and fell progressively thereafter. Importantly, the ALT activity never returned to baseline in these animals, remaining at least two to three times above normal throughout the experiment. B cell-depleted splenocytes demonstrated disease kinetics comparable with that seen after total cell transfer. Similarly, $CD4^+$ subset-depleted splenocytes caused acute elevation of serum ALT activity within 7 days after the transfer, and the animals developed persistent liver disease, although the peak of disease activity was lower than that seen after total cell transfer. In contrast, $CD8^+$ subset depletion markedly reduced the peak and diminished the disease activity in the chronic phase later than 7 days. In addition, we assume that a contaminating 1.4% ($1.3 \times 10^6$) of $CD8^+$ T cells in this $CD8^+$ subset-depleted population may not influence the kinetics of liver disease, because we observed that transfer of $1 \times 10^7$ total splenocytes, which contained ~20% ($2 \times 10^6$) $CD8^+$ T cells, did not cause elevation of ALT in this model.[4]

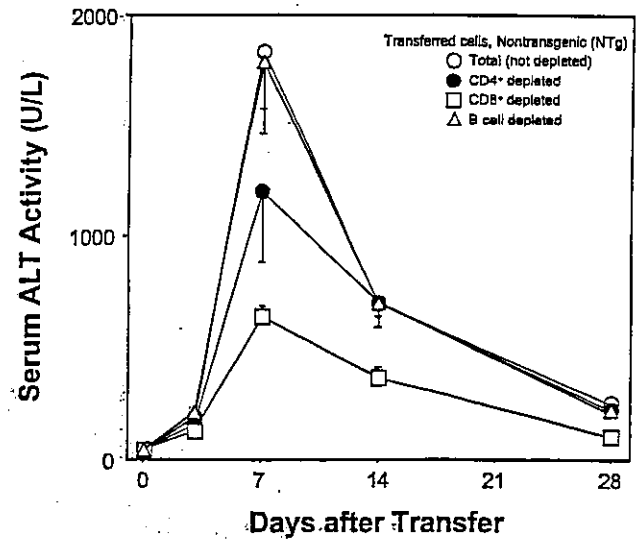


Fig. 1. Kinetics of serum alanine aminotransferase (*ALT*) after transfer of $CD4^+$ T cell-depleted, $CD8^+$ T cell-depleted, or B cell-depleted splenocytes in a transgenic mouse model of chronic hepatitis B. The splenocytes were obtained from hepatitis B surface antigen-primed, syngeneic nontransgenic mice. Nine $\times$ $10^7$ cells of the splenocytes depleted of $CD4^+$ [$CD4^+$, 1.4%; $CD8^+$, 20.8%; B ($CD19^+$), 32.4%], $CD8^+$ ($CD4^+$, 15.0%; $CD8^+$, 1.4%; B, 28.5%), or B cells ($CD4^+$, 17.5%; $CD8^+$, 38.5%; B, 0.1%) were transferred into hepatitis B virus transgenic mice. At the same time, transfer of the total splenocytes ($1 \times 10^8$ cells; $CD4^+$, 12.7%; $CD8^+$, 16.7%; B, 26.8%) was performed for control purposes. The serum ALT activity (mean units/liter) was monitored to evaluate liver injury; *bars*, ±SE. Each group represents 5 animals.

Consistent with the differences in the kinetics of liver disease induced by the subset-depleted cells, transfer of $CD8^+$ subset-enriched splenocytes displayed the prolonged kinetics comparable with total cell transfer except for the lower peak of ALT (Fig. 2). In contrast, $CD4^+$ subset-enriched cells caused a transient elevation of ALT 7 days after adoptive transfer that seemed to improve 14 days after the transfer. In addition, we confirmed that transgenic splenocytes induce no disease in the recipient mice, indicating that all subsets of transgenic splenocytes are perfectly immunologically tolerant to the viral antigens as observed previously (21). Whereas these subset-enriched splenocytes included unidentified non-T and non-B cells that might influence the kinetics of liver disease, the data collectively demonstrate that $CD8^+$ T lymphocytes contributed not